2017 Vol. 5, No. 2

Minnesota Academy of Science Journal of Student Research

Promoters of Melanoma Metastasis Cancer and Tick-borne Bacteria: Identification of *Bartonella henselae* and *Borrelia burgdorferi* as Possible

M. Scott and C. Maxwell
Breck School, Minneapolis, MN

Melanoma is one of the deadliest cancers in the world, killing over 10,000 Americans every year. However, in melanoma's earliest stages, nearly all patients can be successfully treated. Because of this discrepancy, the purpose of this study was to look at possible environmental factors that induce melanoma metastasis in its most crucial, early stages.

This study identified *Bartonella henselae*, a tick-borne bacteria most known for causing cat-scratch disease, as a possible promoter of melanoma metastasis. *Bartonella henselae* is most common in the Pacific Northwest, a region disproportionately affected by melanoma. Additionally, through a process called angiogenesis, *Bartonella henselae* up-regulates the formation of blood and lymph vessels. This study hypothesized that vessels formed by *Bartonella henselae* infection can carry essential nutrients and oxygen to cancerous tumors, exacerbating the speed at which malignancies spread throughout the body, making melanoma more deadly. As a secondary focus, this study also looked at the role of *Borrelia burgdorferi*, another tick-borne bacteria that causes Lyme disease, because of the high frequency of *Bartonella henselae* and *Borrelia burgdorferi* co-infections. Using immunohistochemistry staining and confocal microscopy, the presence of *Bartonella henselae* and *Borrelia burgdorferi* were examined and discovered in melanoma samples for the first time. Additionally, *Bartonella henselae* was found to cluster around lymphatic vessels in the melanoma samples, which is necessary for the induction of angiogenesis.

This study suggests that the relationship between *Bartonella henselae* and vasculature in melanoma should be further investigated in determining what function tick-borne bacteria have in influencing melanoma metastasis. As it becomes clear what role these bacterial infections play in cancer, better treatment plans and more accurate prognoses can be developed for melanoma and cancer patients throughout the world.

Keywords: melanoma, *Bartonella,* cancer, angiogenesis, VEGF, imaging
Abbreviations: ultraviolet (UV), vascular endothelial growth factor (VEGF), phosphate-buffered saline (PBS), trisphosphate-buffered saline (TPBS), Optimal Cutting Temperature (OCT)

Funding and resources were provided by the University of Minnesota Tissue Imaging Laboratory.

This paper received a 2017 Minnesota Academy of Science STEM Communicator Award. The judging process for this award satisfied the function of manuscript review.

INTRODUCTION AND GOALS

Melanoma is a critical health issue, with nearly 77,000 cases and over 10,000 fatalities expected in the United States this year (1). Despite advancements in decreasing the mortality rate and extending the life expectancy for patients with this cancer, the number of melanoma cases has doubled in the last three decades (2). Melanoma is the deadliest form of skin cancer and becomes practically untreatable once it metastasizes throughout the entire body. Because current research is making comparatively little progress, additional factors that induce melanoma formation must be investigated in order to develop better, more effective treatments (1).

The mechanisms of melanoma metastasis have been heavily researched and are well understood. Malignant melanocytes — the cells found between the dermis and epidermis that produce skin pigmentation — proliferate uncontrollably and accumulate into melanoma tumors. During their localized stage of growth, tumors can be surgically removed, garnering a survival rate of 92%. However, once the cancer enters the red blood vessels and lymph nodes and metastasizes throughout the body, the survival rate of melanoma decreases to 17%. Because of this, early detection and removal of cancerous growths are essential (1).

The most common cause of melanoma is overexposure to ultraviolet (UV) radiation, which accounts for nearly 65% of melanoma cases. (3) UV radiation induces genetic mutations in melanocytes that lead to their uncontrolled spreading throughout the entire body. Due to the unequal distribution of UV radiation from the sun across the surface of the earth and the disproportionate effect of UV radiation on Caucasians, melanoma rates vary geographically. Surprisingly, the Pacific Northwest has some of the highest melanoma rates in the country (3). Oregon, a state that receives less sunshine annually than 46 of the other 50 U.S. states, is consistently in the top five states ranked for melanoma rates. It also has a melanoma mortality rate greater than the national average (3). The discrepancy between melanoma rates and amount of sun, which contemporary science supports as the cause of melanoma, points to the role of additional factors, possibly environmental ones, that contributes to melanoma formation. The purpose of this study is to investigate if *Bartonella henselae*, a species of a tick-borne gram-negative bacteria found in the Pacific Northwest, induces melanoma formation and metastasis.

Bartonella henselae has been shown to share several traits, such as 25 and inflammation, with that of bacterial infections that cause cancer (5). We aim to better understand how external environmental factors, like *Bartonella henselae*, may influence melanoma growth so that more effective treatment and prevention plans can be developed.

Bartonella henselae was first discovered as the causative agent of cat-scratch disease. Since then, diagnoses of *Bartonellosis* (infections *of Bartonella henselae*) have numbered over 20,000 people every year in the United States (5). Common symptoms of *Bartonella henselae* infections include rash, fatigue, headache, and lymphadenopathy, a disease in which the lymph nodes swell abnormally due to an inflammatory response (6). *Bartonella henselae* is transmitted to humans through a reservoir host, commonly a cat that has been inoculated with the bacteria by a blood-sucking vector such as a ticks, fleas, or lice. It is suspected that between 25–40% of all cats carry *Bartonella henselae* at some point in their lifetime, which speaks to the prevalence of *Bartonella henselae* (6).

Bartonella henselae uses its host's cells to prevent an immune system response, rendering it difficult to eradicate. Because of *Bartonella henselae's* slow reproduction time of 21–22 hours, symptoms often occur several days or weeks after infection. Additionally, *Bartonella henselae's* ability to evade detection even by advanced lab tests means it is often left undiagnosed (7). Given that the symptoms patients exhibit are very general and that *Bartonella henselae* is so difficult to detect, it is estimated that only 1% of *Bartonella henselae* infections are diagnosed and reported. When left undiagnosed, *Bartonellosis* can lead to prolonged and persistent infections that often manifest into more advanced symptoms in humans, including neurocognitive impairment, bone damage, and internal organ inflammation (8). Persistent infection is most often seen in immunocompromised patients, such as those with AIDS; however, it is also common to see persistent infection in healthy individuals (9).

In humans, *Bartonella henselae* is a promoter of angiogenesis, the formation of endothelial cells that make up blood vessels. Angiogenesis is integral to melanoma metastasis, as it provides tumors a source of oxygen and nutrients (10). When *Bartonella henselae* Adhesin A, an appendage located on the outer membrane of *Bartonella henselae*, adheres to the surface of endothelial cells, the pathogen stimulates the production of vascular endothelial growth factor A (VEGF-A) and vascular endothelial growth factor B (VEGF-B). These cytokine growth factors stimulate the formation of red blood vessels from existing vessels, and promote the survival of existing vessels (11). In the case of melanoma, angiogenesis is required for the invasion of melanocytes into the lymph and blood vessels, a state known as the "vertical growth phase" (10). Due to the role of angiogenesis in melanoma, we hypothesized the *Bartonella henselae's* ability to induce VEGF production will accelerate melanoma metastasis.

Additionally, *Bartonella henselae* is known to cause lymphadenitis, the inflammation of lymph nodes, and induce lymphangiogenesis, the growth of lymph vessels, in *in vitro* studies.

Melanoma metastasis to the lymph nodes significantly decreases the survival rate of melanoma patients, and lymphangiogenesis has been shown to secrete a chemotactic protein that increases the speed of melanoma metastasis. (11) Because of *Bartonella henselae's* ability to induce lymphangiogenesis, we also hypothesized that *Bartonella henselae*'s interaction with the lymph nodes and lymph vessels possibly increases the rate at which melanoma metastasizes. Finally, persistent infections can cause changes in cells' DNA that lead to cancer over time (12). Similar to other carcinogenic bacteria, such as *Helicobacter pylori*, persistent infection is common for many people with *Bartonellosis* (7*).*

Due to the prevalence of co-infections of *Bartonella henselae* with other tick-borne diseases, this study also looked at *Borrelia burgdorferi*, a genus of bacteria that causes Lyme disease, as a secondary focus (14). Lyme disease is chronic, and treatment often fails to prevent relapsing infection. Additionally, previous studies have shown possible correlations between *Borrelia burgdorferi* and cancers such as non-Hodgkin Lymphoma (20).

The main goal of our study was to determine what role *Bartonella henselae* plays in exacerbating the spread of melanoma by imaging melanoma tissue samples of *Bartonella henselae*-positive patients. The secondary goal of this study was examining the possible role of *Borrelia burgdorferi* in the same samples. Using immunostaining and confocal microscopy, we were able to directly observe *Bartonella henselae* and *Borrelia burgdorferi* immunoreactivity in melanoma tissue samples and the biological structures the bacteria interacted with, such as lymphatic vessels. The samples that we tested were biopsied from melanoma patients whose blood samples tested positive for *Bartonella henselae* in an Oregon hospital.

We decided to use confocal imaging over other techniques as *Bartonella henselae* is often undetected in typical diagnosis tests. When these tests have failed, confocal microscopy has been shown to detect *Bartonella henselae.* For this reason, confocal microscopy was used to conclusively determine whether the melanoma samples were infected with *Bartonella henselae*. Additionally, using immunohistochemistry staining we were able to highlight different biological structures such as lymphatic vessels, blood vessels, and VEGF as well as *Bartonella henselae*. In this type of staining protocol, primary antibodies are first used to stain specific antigens and proteins. Secondary antibodies, which are conjugated to fluorophores, bind to primary antibodies and fluoresce to show the location of different biological structures. (13).

MATERIALS

Melanoma tissue samples were obtained from North Carolina State University (Asheville, NC), though originally biopsied from patients in Oregon. These samples were initially sectioned for other reasons than this study and were then de-identified before use in our study. Control skin samples were obtained from the University of Minnesota (Minneapolis, MN). Secondary antibodies and nuclear stains were obtained from Jackson ImmunoResearch (West Grove, PA), while primary antibodies were obtained from Immunostar Research (Madison, WI).

All imaging was carried out using an Olympus FV1000 BX2 Confocal Microscope and processed using Olympus FLUOVIEW software, both of which were purchased from Nikon (Tokyo, Japan).

Additional imaging analysis was done using Fiji software developed by the Laboratory for Optical and Computational Instrumentation at the University of Wisconsin-Madison (Madison, WI).

METHODS

Deparaffinization of samples

Six metastatic melanoma biopsies were obtained from two patient donors infected with *Bartonella henselae*. A section of each biopsy was first cut using a scalpel and then incubated overnight at 35 ºC to increase the viscosity of the surrounding paraffin. To deparaffinize and rehydrate the samples, the samples were then rinsed in xylene and immersed in a series of ethyl alcohol washes of increasing dilution. Each wash lasted 30 minutes long, and the entire process was repeated multiple times to ensure that all paraffin was removed from the samples. After this, samples were left in phosphate-buffered saline (PBS) overnight.

Sectioning of samples

Prepared samples were cut into thinner sections to ensure proper staining. The six melanoma samples and two control skin samples were each placed onto a mounting stand and loaded into a cryostat at -30 ºC. To mount the samples, they were embedded in an Optimal Cutting Temperature compound (OCT), which solidified around the sample. Then, the mounting stand was secured and the cutting blade was loaded into the cryostat. Sections 40 μm in length were cut and placed into a well of eight Pyrex 9-well glass plates pre-filled with PBS. The PBS was subsequently replaced with 5% normal serum in triphosphate-buffered saline (NTPBS), and the samples were incubated overnight at room temperature with light gyro shaking.

In total, there were 16 plates, each with three different melanoma samples and one control skin sample. Plates 1–8 received melanoma samples with catalogue numbers M5231, M5232, and M5233, while Plates 9-16 received melanoma samples A1, A2, and A3 Immunohistochemical staining

The staining protocol used in this study was adapted from a previous protocol used to identify *Bartonella henselae* and *Borrelia burgdorferi* (15). On the first day of staining, the 5% NTPBS that the samples were deparaffinated in (or something similar) was replaced with 200 μL of tris-phosphate buffered saline (TPBS) and incubated for 3 hours at room temperature with light gyro-shaking. After this, the TPBS solution was removed and primary antibodies were added to each of the plates. Plates 1–7 and 9–13 each received a different combination of primary antibodies, which can be seen Table 1. Plates 8 and 14–16 received PBS diluted at a 1:400 dilution in TPBS. After the primary antibodies were added to each of the plates, the samples were incubated overnight at room temperature with light gyro shaking.

The samples were washed with TPBS then re-washed five hours later. Subsequently, the TPBS was decanted, and 1% NTPBS was added to all plates. The samples were again incubated overnight at room temperature with gentle gyro rotation. Secondary antibodies were applied to Plates 1–7 and 9–15. Plates 8 & 16 did received PBS diluted at a 1:400 dilution in TPBS. Each secondary antibody, conjugated to a fluorophore, emitted fluorescence when bound to a primary antibody and exposed to the corresponding laser. The specificity of a secondary antibody to a primary antibody was dependent on the host species that the primary antibody was produced in. To ensure that there was non-specific binding, each secondary antibody in a plate was specific to only one primary antibody. To distinguish different structures within the samples, the secondary antibodies in each plate were chosen to emit different colored fluorescence. Alexa Fluor conjugated 488, Alexa Fluor conjugated 594/Cy3, and Alexa Fluor conjugated 647 emit green, red, and far-red fluorescence, respectively.

DAPI, which emits blue fluorescence, was applied to Plates 1–7 and 9–14. PBS was added to Plates 8 and 15–16 as a negative control. In Plate 16, a sham solution composed of 1:100 PBS was added for both secondary and primary antibody antibodies. After incubating the samples for eight hours, the tissue samples were washed twice with PBS for 30 minutes each as a final preparation before they were mounted onto their cover slips.

Table 1. The primary antibodies, secondary antibodies, and nuclear stains used in each well. The “Primary antibodies” column lists the host species each primary antibody was derived from and the antigen specific to that antibody. The “Secondary antibodies” lists the host species specificity of each secondary antibody and their conjugated fluorophore. A “-“ denotes that a negative control solution was added to that plate.

Plate	Primary antibodies	Secondary antibodies	Nuclear stain
Plate 1	(Goat) VEGF-C (Chicken) *Bartonella henselae* (Mouse) *Borrelia burgdorferi*	(Goat) Alexa Fluor 488 (Chicken) Alexa Fluor 594 (Mouse) Alexa Fluor 647	DAPI
Plate 2	(Goat) Lyve 1 (Chicken) *Bartonella* (Mouse) *Borrelia*	(Goat) Alexa Fluor 488 (Chicken) Alexa Fluor 594 (Mouse) Alexa Fluor 647	DAPI
Plate 3	(Rabbit) Collagen Type 4 (Chicken) *Bartonella* 53 (Mouse) *Borrelia*	(Goat) Alexa Fluor 488 (Chicken) Alexa Fluor 594 (Mouse) Alexa Fluor 647	DAPI
Plate 4	(Goat) VEGF-C (Chicken) *Bartonella* 53 (Mouse) Melanocyte-5	(Goat) Alexa Fluor 488 (Chicken) Alexa Fluor 594 (Mouse) Alexa Fluor 647	DAPI
Plate 5	(Goat) Lyve-1 (Chicken) *Bartonella* 53 (Mouse) Melanocyte-55	(Goat) Alexa Fluor 488 (Chicken) Alexa Fluor 594 (Mouse) Alexa Fluor 647	DAPI
Plate 6	(Rabbit) Collagen Type 4 (Chicken) *Bartonella* 53 (Mouse) Melanocyte-5	(Goat) Alexa Fluor 488 (Chicken) Alexa Fluor 594 (Mouse) Alexa Fluor 647	DAPI
Plate 7 (Secondary Control)	--	(Goat) Alexa Fluor 488 (Chicken) Alexa Fluor 594 (Mouse) Alexa Fluor 647	--
Plate 8 (Control)	--	--	--
Plate 9	(Mouse) *Bartonella* (Rabbit) Collagen Type 4 (Goat) Lyve-1	(Mouse) 488 (Rabbit) Cy3 (Goat) 647	DAPI
Plate 10	(Mouse) *Borrelia* (Rabbit) Collagen Type 4 (Goat) Lyve 1	(Mouse) 488 (Rabbit) Cy3 (Goat) 647	DAPI
Plate 11	(Chicken) *Bartonella* 53 (Rabbit) Collagen Type 4 (Goat) Lyve 1	(Goat) 488 (Chicken) 657 (Rabbit) Cy3	DAPI
Plate 12	(Chicken) *Bartonella* (Rabbit) Collagen Type 4 (Goat) VEGF-C	(Goat) 488 (Chicken) 657 (Rabbit) Cy3	DAPI
Plate 13	(Chicken) *Bartonella* (Rabbit) Lyve 1 (Goat) VEGF-C	(Goat) 488 (Chicken) 657 (Rabbit) Cy3	DAPI
Plate 14 (Secondary Control)	--	(Mouse) 488 (Rabbit) Cy3 (Goat) 647	--
Plate 15 (Secondary Control)	--	Goat) 488 (Chicken) 657 (Rabbit) Cy3	--
Plate 16 (Control)	--	--	--

Sample Counting

After staining, the samples were prepared for imaging. To mount the samples to the coverslips, each tissue section was placed on the coverslip, positioned so that there were no overlaps in the tissue, and immersed in a bubble of agar. The excess agar was then pipetted away. Once all nine tissue samples had been properly prepared, they were placed on a ceramic boat, which was immersed in the following for a period of 20 min each: 75% EtOH, 95% EtOH, 100% EtOH, and methyl salicylate. After this cycle, the microscope slide was pretreated with DPX and the coverslip was placed, with the tissue facing down, on the slide's surface. Once the slides were prepared, they were placed on a drying rack in a biological safety cabinet, where they were protected from light.

Preliminary imaging

After the completion of staining and mounting, all samples were imaged using an Olympus BX1000 fluorescence microscope. Images from each sample were taken with DAPI, TXRED (Alexa Fluor 594), FITC (Alexa Fluor 488), and Cy5 filters. After imaging each sample, fluorescence from *Bartonella henselae*, *Borrelia burgdorferi*, lymphatic, and Collagen Type 4 antibody immunoreactivity was examined. Samples that showed presence of a bacterial were selected to be imaged using the confocal microscopy. The samples chosen were sample A1 from Plate 10, sample A3 from Plate 7, and each of their secondary antibody controls. All samples chosen for confocal microscopy came from the same patient.
Confocal microscopy

Confocal microscopy was used to identify regions of samples that were infected with either *Bartonella henselae* and *Borrelia burgdorferi*. To detect possible areas of infection, the slides chosen from the preliminary immunohistochemistry staining were positioned on the microscope stage, and the confocal microscope was set to "Transmitted Light" (Brightfield) emission. Using an Olympus 4x zoom objective, samples were then observed in the microscope binoculars and positioned so that the epidermal-dermal boundary of the samples was clear. At this point, the microscope was switched from Brightfield emission to fluorescence emission, and the objective was switched to a higher power 40x zoom objective. In the Olympus FLUOVIEW software, dyes (channels that receive fluorescence signals) were selected for each of the four secondary antibodies based on their wavelength emission. Four lasers with excitation wavelengths that corresponded with each of the four secondary antibodies were turned on. To confirm that fluorescence from one channel was not bleeding into another, the powering on of lasers was staggered. Lasers were set at 20–30% power to prevent photobleaching that could damage the antibodies and stains.

After powering each laser and channel, the samples could be viewed confocally in FLUOVIEW by selecting XY repeat. To find a region of a sample to image, the microscope controller was used to move the stage, and the sample was observed for fluorescence from either *Borrelia burgdorferi* or *Bartonella henselae* immunoreactivity. After finding an area to image, the microscope's XYZ mode, which can penetrate through the samples, was used to record a set of 49 images at different depths in the sample. The images, each 0.55 μm in thickness, were subsequently combined into a 3-dimensional model of the sample. The resulting image was then examined for regions infected with either *Bartonella henselae* and *Borrelia burgdorferi* by looking for intense fluorescence from bacterial immunoreactivity. Additional images were taken with a higher power UNAPLO 60x zoom oil objective following the imaging protocol.

ANALYSIS

Due to the small patient sample size of this study, a descriptive analysis was used rather than a statistical analysis. To determine whether fluorescence came from *Bartonella henselae* or *Borrelia burgdorferi* immunoreactivity, samples were compared with their respective secondary control. The location of *Bartonella henselae* and *Borrelia burgdorferi* immunoreactivity with respect to lymphatic vessels and other biological structures was also noted. All analysis was done using FIJI image analysis software.

RESULTS

After preliminary imaging, a section of melanoma sample "A1" stained in Plate 10 (Fig. 1), a section of melanoma sample "A3" stained in Plate 13 (Fig. 3), and both of their secondary controls (Fig. 2 & 4) were

chosen for confocal microscopy imaging. The A1 section was stained for *Borrelia burgdorferi*, collagen type IV, and lymphatic immunoreactivity, while the A3 section was stained for *Bartonella henselae*, VEGF-C, and lymphatic immunoreactivity. No primary antibodies or stains were added to the secondary controls, so we could determine whether fluorescence was from endogenous sources (auto-fluorescence) or from the staining.

Figure 1 shows a section from melanoma sample A1 imaged using using an Olympus 60x zoom objective and magnified 2.5x post imaging. *Borrelia burgdorferi* immunoreactivity was detected and denoted in yellow boxes, as seen in Panel A. Red fluorescence denotes lymphatic immunoreactivity from Alexa Fluor 488. Green fluorescence denotes *Borrelia burgdorferi* immunoreactivity from Alexa Fluor 647. Cyan fluorescence denotes nucleated cell immunoreactivity from DAPI stain. Panel B depicts a 3-dimensional representation of the image.

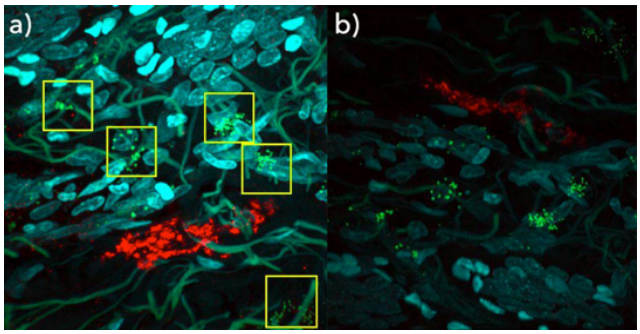

Figure 1. Borrelia burgdorferi Immunoreactivity detected in melanoma section from sample Panel A shows a z-stack projection of *Borrelia burgdorferi* immunoreactivity (yellow boxes). Panel B shows a 3-dimensional model of the sample area.

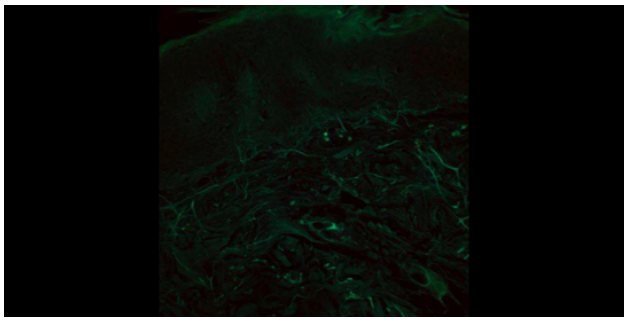

Figure 2. No *Borrelia burgdorferi* immunoreactivity detected in secondary control of sampleA1. Section of an A1 melanoma imaged using a UNAPLO 40X zoom objective. No *Borrelia burgdorferi* immunoreactivity was detected in z-stack projection (secondary antibody control).

Figure 2 shows a section from melanoma sample A1 imaged using an Olympus 40x zoom objective. No *Borrelia burgdorferi* immunoreactivity was detected (secondary control).

Figure 3 shows a section from melanoma sample A3 imaged using using a UNAPLO 60x zoom oil objective and magnified 2.5x post imaging. *Bartonella henselae* immunoreactivity was detected and denoted by yellow boxes, as seen in Panel A of Figure 3. Red fluorescence denotes lymphatic immunoreactivity, and Green fluorescence denotes *Borrelia burgdorferi* immunoreactivity. The DAPI VEGF-C/Alexa Fluor 488 channels were removed post-imaging to improve clarity. Panel B depicts a 3-dimensional representation of the image.

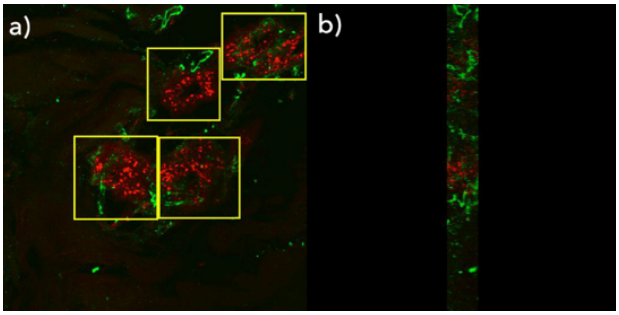

Figure 3. *Bartonella henselae* Immunoreactivity detected in melanoma section from sample "A3". Section was imaged using an Olympus 60x zoom objective and magnified 2.5x post imaging. Panel A shows a z-stack projection of *Bartonella henselae* immunoreactivity and lymphatic immunoreactivity (yellow boxes). Panel B shows a 3-dimensional model of the sample area.

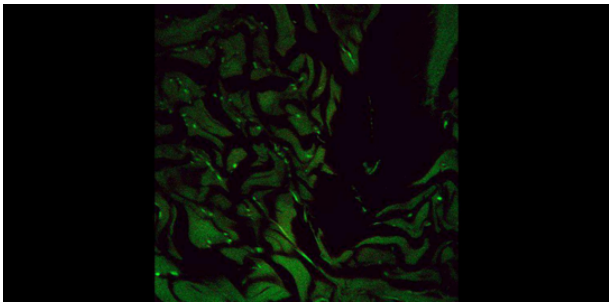

Figure 4. No *Bartonella henselae* immunoreactivity detected in the secondary control of sample "A3". Section was imaged using an Olympus 40x zoom objective. No *Bartonella henselae* immunoreactivity was detected in z-stack projection (secondary antibody control).

Figure 4 shows a section from melanoma sample A3 imaged using using an Olympus 40x zoom objective. No *Bartonella henselae* immunoreactivity was detected in the z-stack projection (secondary control).

DISCUSSION

After imaging with confocal microscopy, A1 was found to contain several clusters of *Borrelia burgdorferi* immunoreactivity; however, these areas appeared to have no preference to form around the lymphatic vessels. This could be seen in both the z-stack and three-dimensional projections of the sample. The *Borrelia burgdorferi* immunoreactivity was small and round in shape. This is atypical as *Borrelia burgdorferi* is most often spiral-shaped and long (up to 20 µm in length), suggesting that the *Borrelia burgdorferi* in this sample exhibited a less common phenotype, most likely its cystic form, which is rounder in shape and can cause persistent infection (18,19). Staining from the collagen type 4/ Cy3 antibodies was unable to be analyzed, as it produced highly speckled and scattered fluorescence, so this channel was removed from the final images included in this study and was. Imaging of this sample's secondary control showed no regions of intense fluorescence, meaning that all fluorescence in this sample came from immunoreactivity. In sample "A3," regions of *Bartonella henselae* immunoreactivity were evident in several different areas surrounding lymphatic vessel immunoreactivity. This could be seen in both the z-stack and three-dimensional projections of the sample. Additionally, *Bartonella henselae* immunoreactivity fluorescence formed long strips and clusters around the lymphatic vessels, which are signs of bacterial biofilms. This finding was consistent with that of Chomel et al. (2009), which attributed *Bartonella henselae* biofilm formation to persistent infection of *Bartonella henselae* (16). Additionally, these clusters are possible indicators of lymphangiogenesis, as *Bartonella henselae* forms around lymphatic vessels during lymphangiogenesis's initial stages (11).

Lymphangiogenesis, the growth of lymphatic vessels from pre-existing vessels, is an important step in melanoma metastasis, as it allows melanoma tumors to spread to lymph nodes (21). This finding supports our hypothesis that angiogenesis caused by *Bartonella henselae* could potentially accelerate melanoma metastasis. Sample "A3" was compared with its secondary control, and no areas of intense fluorescence were detectable. Fluorescence from DAPI and VEGF-C/Alexa Fluor 488 were removed from the final images included in this paper to increase clarity.

CONCLUSIONS

We successfully stained melanoma samples using immunohistochemistry staining and imaged using confocal microscopy. We also successfully detected *Borrelia burgdorferi* and *Bartonella henselae* immunoreactivity from the samples imaged. This study suggests that understanding the relationship between *Bartonella henselae* and lymphatic vessels in melanoma should be further pursued, as it was shown that *Bartonella henselae* clustered around lymphatic vessels, a possible sign of lymphangiogenesis. To our knowledge, this study is the first of which to examine and detect *Bartonella henselae* and *Borrelia burgdorferi* immunoreactivity in melanoma samples. Identifying the presence of these bacteria in melanoma is an important step in determining what role they bacteria play in the growth of melanoma.

Sources of Error and Future Work

A limitation of this study was that staining from Collagen Type IV primary antibodies produced scattered and unfocused fluorescence. Because of this, the interaction between *Bartonella henselae* and *Borrelia burgdorferi* with red blood vessels was unable be explored in this study, as Collagen Type IV antibodies are specific to red blood vessels. Poor fluorescence most likely was a result the age of the Collagen Type IV secondary antibody used in this study, which lost specificity to red blood vessels. Future work should involve staining new sections of the samples used in this study with a fresher Collagen Type IV secondary antibody. Additionally, only two biopsies from one patient were imaged with the confocal microscope, as we did not have access to more a robust pool of patients. Although this study showed *Bartonella henselae's* presence in melanoma, having more samples would allow us to more conclusively determine what ways *Bartonella henselae* and *Borrelia burgdorferi* affect melanoma growth.

In the future, more melanoma samples from patients who have tested positive for *Bartonella henselae* and *Borrelia burgdorferi* or have symptoms of these tick-borne infections should be imaged. To obtain melanoma samples, a survey will be send to prospective participants inquiring about their exposure to tick-borne illnesses and cats (the most common reservoir host of *Bartonella henselae*).

Samples from patients who have previously tested negative serologically for *Bartonella henselae* will also be included in our future work. The other samples stained in this study will be imaged confocally, as well.

Additionally, the relationship between *Bartonella henselae* and melanoma at a molecular level will be further investigated. A co-culture will be performed to examine what effect *Bartonella henselae* has on the malignancy of melanoma cells. A microRNA analysis, which can measure the prevalence of different miRNA responsible for cancer expression, will then be used to determine what mechanisms of melanoma are influenced by Bartonella henselae. Melanoma is responsible for the deaths of thousands of people every year; however, by developing a deeper understanding of what factors influence melanoma's formation and metastasis, many deaths can be prevented. This study's findings support the growing recognition of the environment's role in cancer. Because the process of angiogenesis is integral to tumor formation in all metastatic cancers, this research can be applied to other cancers as well. As it becomes clear what role bacterial infections play in cancer, better treatment plans and more accurate prognoses can be developed for melanoma and cancer patients throughout the world.

ACKNOWLEDGEMENTS

First, we would like to thank our parents for the love and support they've showered us with from the beginning. We would like to thank Dr. Marna Ericson, Director of the Cutaneous Imaging Lab at the University of Minnesota, for providing resources and training for immunostaining and imaging, and especially for serving as the advisor of this project. The University of Minnesota Cutaneous Imaging Lab provided support to this study, and the University of Minnesota Imaging Center provided access to their imaging resources. Thank you also to Dr. Balakrishnan, Research Associate at the North Carolina State University, for supplying us with melanoma tissue samples used for staining. We especially would like to thank Ms. Princesa Hansen for the valuable guidance and support. Lastly, to unnamed friends and family who have been encouraging and helped us see this project through, thank you, we couldn't have done it without you.

REFERENCES

1. American Cancer Society. Melanoma Skin Cancer. http://www.cancer.org/acs/groups/cid/documents/webcontent/003120-pdf.pdf Published May 5, 2016, accessed May 27, 2016.

2. Center for Disease Control. Rates of new melanomas – deadly skin cancers – have doubled over last three decades. http://www.cdc.gov/media/releases/2015/p0602-melanoma-cancer.html. Published June 2, 2016, accessed May 30, 2016.

3. Center for Disease Control. What is Skin Cancer? http://www.cdc.gov/cancer/skin/basic_info/what-is-skin-cancer.htm Published 2012, accessed July 26. 2016

4. Jameson P, Greene C, Regnery R, Dryden M, Marks A, Brown J, Cooper J, Glaus B, Greene R. Prevalence of *Bartonella henselae* henselae antibodies in pet cats throughout regions of North America. The Journal for Infectious Disease. 1995; 172(4):1145-1149

5. Jackson L, Perkins B, Wenger J. Cat Scratch Disease in the United States: An Analysis of Three National Databases. American Journal of Public Health. 1993; 83(12):1707–1711

6. Greub G, Raoult D. *Bartonella henselae*: new explanations for old diseases. Society for General microbiology. 2002; 51:915–923

7. Duncan AW, Maggie RG, Breitschwerdt EB. A combined approach for the enhanced detection and isolation of *Bartonella henselae* species in dog blood samples: Pre-enrichment liquid culture followed by PCR and subculture onto agar plates. Journal of Microbiology Methods. 2007; 69:273–281

8. American Cancer Society. Cancer Facts and Figures 2005. Atlanta: American Cancer Society; 2005

9. Breitschwerdt EB, Maggi RG, Nicholson WL, Cherry NA, Woods CW. Bartonella henselae sp. Bacteremia in Patients with Neurological and Neurocognitive Dysfunction. American Society for Microbiology. 2008; 46(9):2856–2861

10. Emmett MS, Dewing D, Pritchard-Jones RO. Angiogenesis and melanoma - from basic science to clinical trials. American Journal of Cancer Research. 2011; 1(7):852–868

11. Harms A, Dehio C. Intruders below the Radar: Molecular Pathogenesis of *Bartonella henselae* spp. Clinical Microbiology Reviews. 2012; 1:1–43.

12. Peppicelli S, Bianchina F, Calorini L. Inflammatory cytokines induce vascular endothelial growth factor-C expression in melanoma associated macrophages and stimulate melanoma lymph node metastasis. Oncology Letters. 2014; 8:1133–1138.

13. Kuper H, Adami HO, Trichopoulos D. Infections as a major preventable cause of human cancer. Journal of Internal Medicine. 2000; 248:171–183.

14. ThermoFisher Scientific. Overview of Immunohistochemistry. https://www.thermofisher.com/us/en/home/life-science/protein-biology/protein-biology-learning-center/protein-biology-resource-library/pierce-protein-methods/overview-immun ohistochemistry.html Published 2016, accessed August 10, 2016.

15. Ericson M. Imaging Tools in Discovery and Development of Phytochemical Chemopreventive Agents. Cancer Prevention. 2014:249-264.

16. LymeDisease.Org. About Lyme Disease Co-Infections. https://www.lymedisease.org/lyme-basics/co-infections/about-co-infections/. Published 2015, accessed August 10, 2016.

17. Chomel BB, Boulouis HJ, Breitschwerd EB, Kasten RW, Taussat MR, Birtles RJ, Koehler JE, Dehio C. Ecological fitness and strategies of adaptation of *Bartonella henselae* species to their hosts and vectors. Veterinary Research. 2009; 40(2):1–22. Journal of Internal Medicine, 2000; 248:171–183.

18. Dombrowski C, Kan W, Motaleb A, Charon N, Goldstein R, Wolgemuth C. The Elastic Basis for the Shape of *Borrelia burgdorferi* burgdorferi. Biophysics Journal. 2009; 96(11): 4409–4417

19. Lantos P, Auwaerter PG, Wormser GP. A Systematic Review of *Borrelia burgdorferi* burgdorferi Morphologic Variants Does Not Support a Role in Chronic Lyme Disease. Clinical Infectious Diseases. 2014; 58(5):663–671

20. Parsonet J. Bacterial Infection as a Cause of Cancer. Environmental Health Perspectives. 1995; 1:263–264.

21. Schadendorf D, Fisher DE, Garbe C, Gershenwald JE, Grob JJ, Halpern A, Herlyn M, Marchetti MA, McArthur G, Ribas A, Roesch A, Hauschild A. Melanoma. Nature Reviews. 2015; 1:1–20.

Additional References

Balakrishnan N, Ericson M, Maggie RG, Breitschwerdt EB. Vasculitis, cerebral infarction and persistent *Bartonella henselae*

henselae infection in a child. Parasistes & Vectors. 2016; 9(284):1–6.

Billeter SA, Levy MG, Chomel BB, Breitschwerdt EB. Vector transmission of *Bartonella henselae* species with emphasis on the potential for tick transmission. Medical and Veterinary Entomology. 2008; 22:1–5.

Breitschwerdt EB, Maggi RG, Cadenas MB, Diniz P. A Groundhog, a Novel *Bartonella henselae* Sequence, and My Father's Death. Emerging Infectious Diseases. 2009; 15(2):2080–2060.

Eicher C, Dehio C. *Bartonella henselae* entry mechanisms into mammalian host cells. Cellular Microbiology. 2012; 14(8):1166–1173.

Ericson M. Imaging Tools in Discovery and Development of Phytochemical Chemopreventive Agents. Cancer Prevention. 2014:249–264.

Gupta P, Sarkar S, Das B, Bhattacharjee S, Tribedi P. Biofilm, pathogenesis and prevention—a journey to break the wall: a review. Arch Microbial. 2016; 198:1–15.

Maggi RG, Mozayenia BR, Pultorak EL, Hegarty BC, Bradley JM, Correa M, Breitschwerdt EB. *Bartonella henselae* spp. Bacteremia and Rheumatic Symptoms in Patients from Lyme Disease–endemic Region. Emerging Infectious Diseases. 2012; 18(5):783–791.

Maggi RG, Ericson M, Mascarelli PE, Bradley JM, Breitschwerdt EB. *Bartonella henselae* henselae bacteremia in a mother and son potentially associated with tick exposure. Parasites & Vectors. 2013; 6:101–110.

Parsonet J. Bacterial Infection as a Cause of Cancer. Environmental Health Perspectives. 1995; 1:263–264.

Schröder G, Schuelein R, Quebatte M, Dehio C. Conjugative DNA transfer into human cells by the VirB/VirD4 type IV secretion system of the bacterial pathogen *Bartonella henselae* henselae. Proceedings of the National Academy of Sciences of the United States of America. 2011; 108(35): 14643